

Pressure Drop Study of Micro-jet Device

Steve Tian Huang
University of Washington
Department of Chemical Engineering
May 30th 2006

Introduction

The micro-jet device was used in Bioengineering laboratory. The simple structure of the device was shown in Fig 1 below.

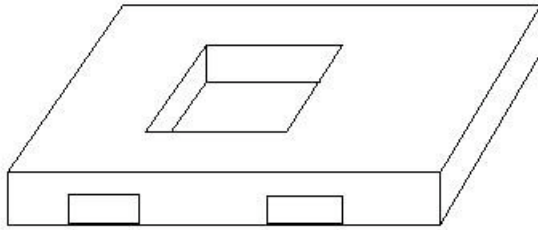


Fig 1. Simple structure of the micro-jet device

There are two side-channels in the device, with an open surface pool located between two side-channels. Side-channels and the pool were connected by micro-jets at the bottom of the device. Fig 2 shows the cross section diagram of the device and how the pool and side-channels were connected.



Fig 2. Cross section diagram of the device

The actual dimension of the device was described in the *Chapter 4: Micro-jets Device* from the handout. In addition, the length of the side-channel was 2 cm and there were 1000 micro-jets distributed evenly along each of the side-channels.

What we were interested in was how the pressure changes and how flow behaves inside the micro-jet device. Also, we want to know about shear stress at certain points because solution with brain cell was used with the device, and cells were sensible to the force generated by the flow.

Objective

The objective of the research was to study the pressure change in various locations in the micro-jet device, and simulate 2D or 3D model in Femlab. And the process of the whole research can be described as 3 steps:

- Pressure Drop Estimation
- 2D simulation
- 3D simulation

Pressure Drop Estimation

1. Pressure drop inside micro-jet

By using equations provided from *Perry's Handbook of Chemical Engineering, 6-12*, pressure changes inside any square channel could be calculated by:

$$\Delta P = \frac{28.5 \cdot \mu \cdot L \cdot v}{a^2}$$

Where 28.5 was constant associated with the square dimension of the channel. The constant could change when the ratio of the length to width of the channel changes.

2. Pressure drop through side-channel

The equation used to calculate the pressure drop in the side-channel was very similar to the one used for micro-jets:

$$\Delta P = \frac{K \cdot \mu \cdot L \cdot Q}{a \cdot b^3}$$

At this equation, the flow rate was used instead of the average velocity. The constant K was determined based on the ratio of a to b. However, the equation can only apply to constant flow rate inside channels. When operating the actual device, the Q, volumetric flow rate was decreasing due to the 1000 micro-jets inside the side-channels. Since we were making the assumption that all the micro-jets were evenly distributed, thus the distances between all the micro-jets must be the same. If we could calculate the pressure drop along each of these small distances between micro-jets, the total pressure drop along the side-channel would be the sum of all the pressure drops through these small distances.

Since all the flow in the side-channel would eventually leave through the micro-jets, we made another assumption that flow rate inside each of the micro-jets were

constant and identical, thus the sum of flow rate inside all the micro-jets were same as the flow getting into the side-channel.

3. Pressure drop due to contraction and expansion

By applying equations from Micro-component flow characterization, the pressure drop can be determined.

For contraction:

$$P_1 - P_2 = \rho \langle v_2 \rangle^2 \left(\frac{27}{35} - \frac{1}{2} \cdot \beta^2 \right) + K_L \cdot \frac{\eta \langle v_2 \rangle}{H_2}$$

For expansion:

$$P_1 - P_2 = \rho \langle v_1 \rangle^2 \left(\frac{27}{35} \cdot \frac{1}{\beta^2} - \frac{1}{2} \right) + K_L \cdot \frac{\eta \langle v_2 \rangle}{H_2}$$

Due to dimension of the device, the constant K_L was determined: $K_L=8$.

Table 1 below shows the sample calculation results.

Table 1. Calculated Pressure Drop in varies location of the device.

Side Channel (psi)	Micro-jet (psi)	Expansion (psi)	Contraction (psi)
2.549e-3	2.452e-3	3.71e-4	3.71e-4

2D simulation

By using the width of the side-channel as the standard length, a 2D model was demonstrated in Femlab. Only one side-channel was described in the model due to the symmetry. Also, there are only 4 micro-jets in the model, instead of 1000. Fig 3 shows the 2D model with 4 micro-jets, with number of degree of freedom of 72915 and number of elements of 14088.

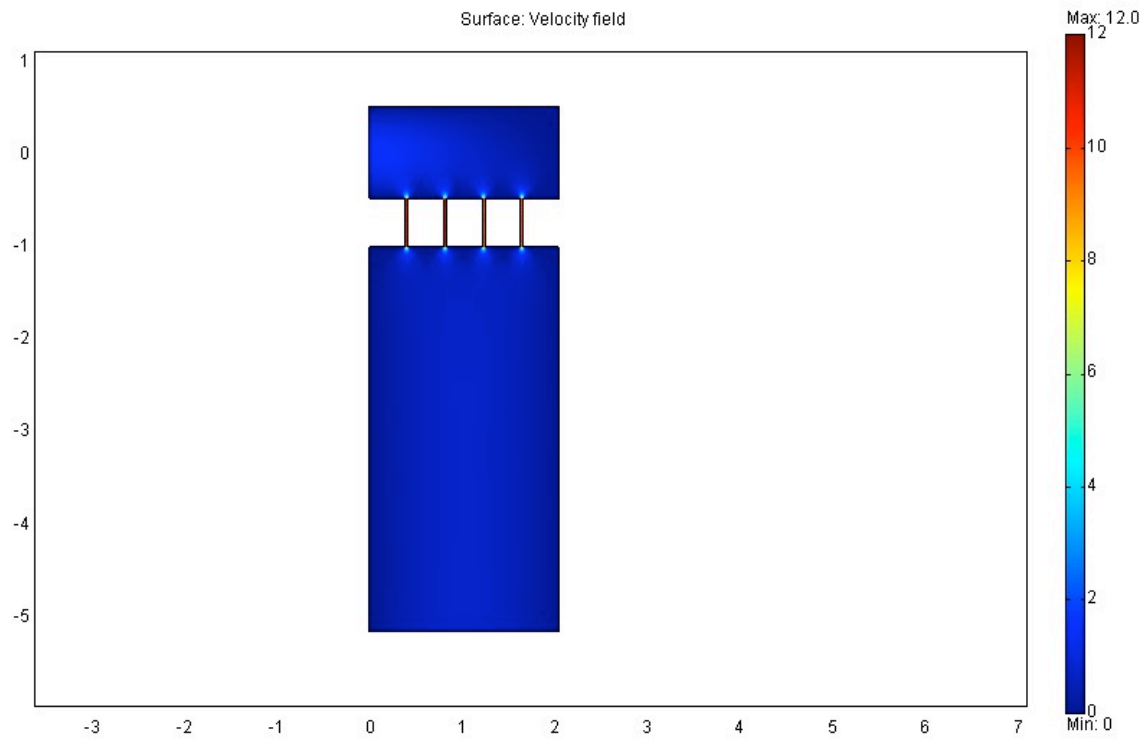


Fig 3. 2D simulation in Femlab

In order to see how the flow behaves through the device, Fig 4 shows the streamline of the model.

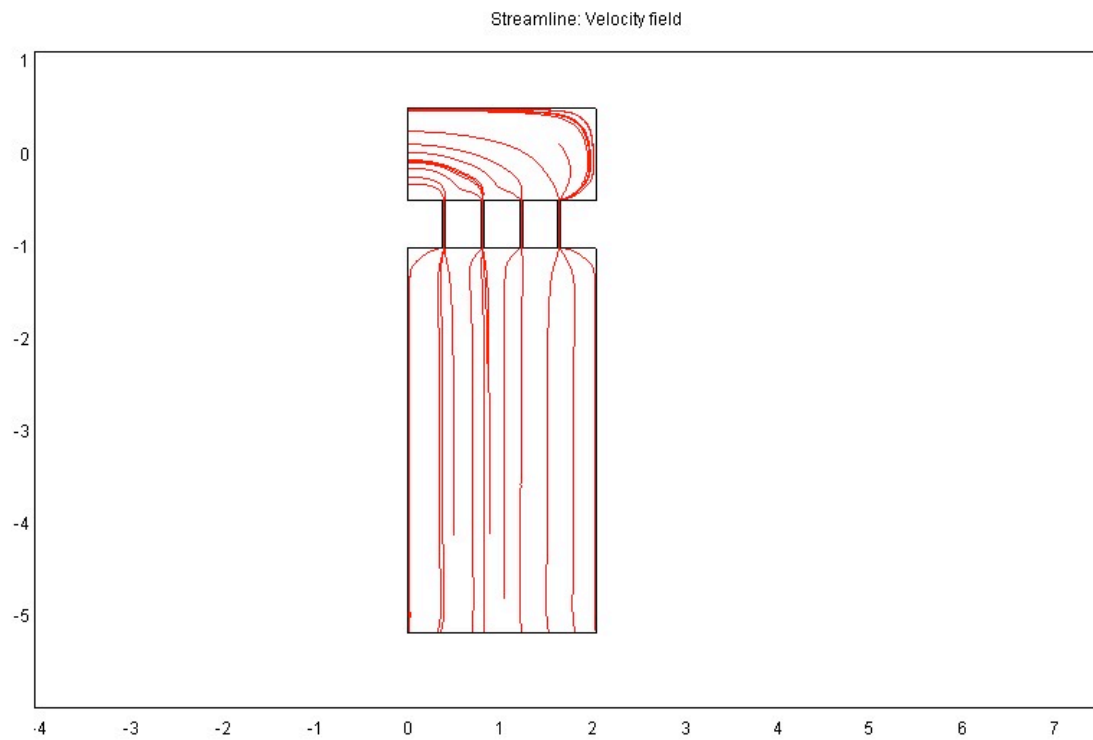


Fig 4. 2D model with streamline

There are two notable points in these graphs. There is a small circulation of flow at the right end of the side-channel, which may cause pressure variance. Also, the relatively straight line at the bottom of the open surface pool predicts that the y-velocity of flow would behave similar to each other around the other end of the pool. This could also prove Professor Folch's prediction. Fig 5 is the plot of pressure vs. position along the centerline of the side-channel.

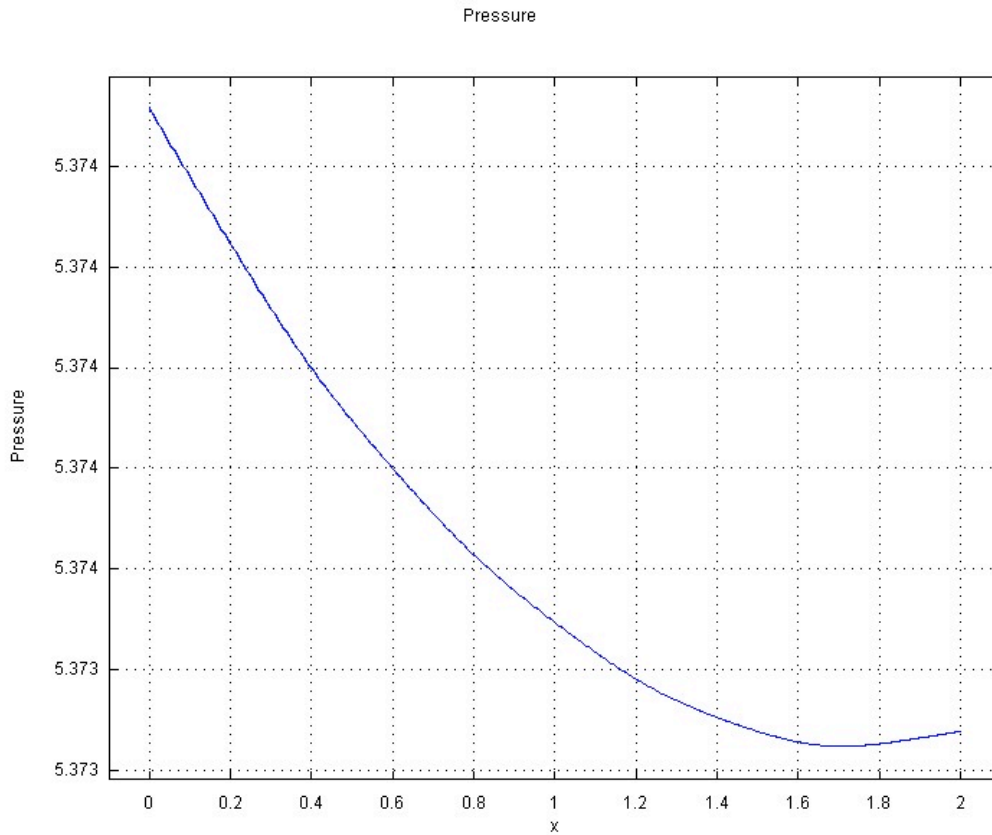


Fig 5. P vs. x along the centerline of the side-channel

The small increase of pressure around the end of side-channel shows the effect of circulation of flow. Fig 6 below plots the velocity vs. position near the other end of the pool.

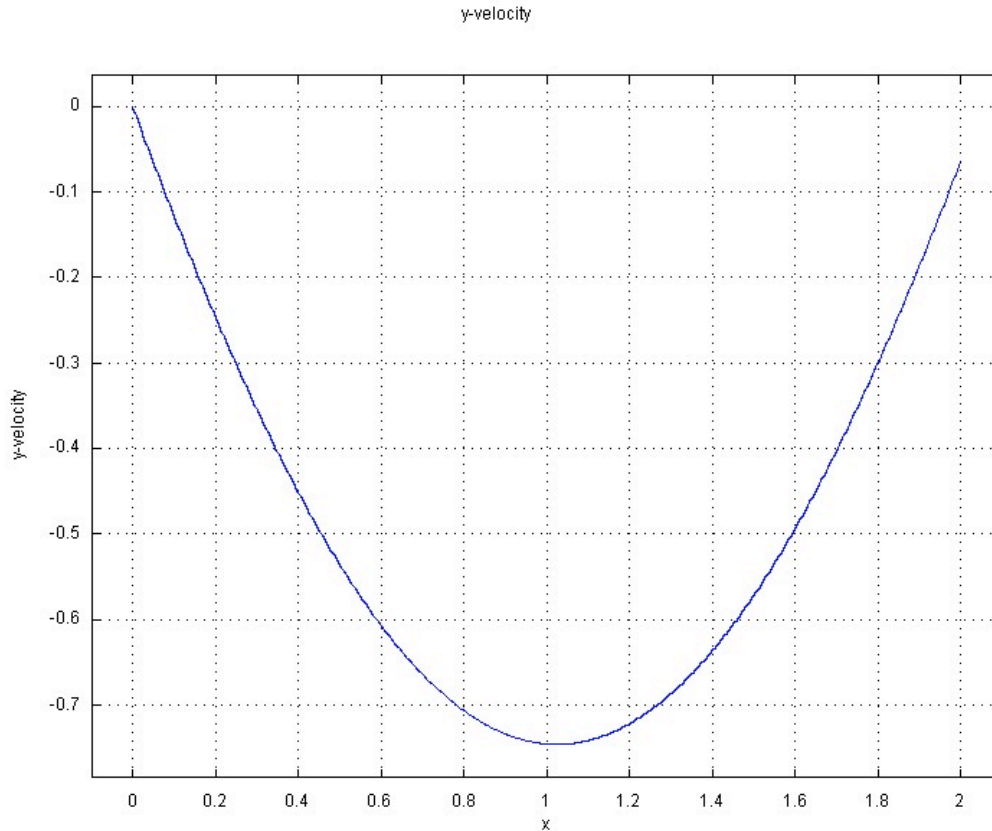


Fig 6. Velocity vs. x-position near the other end of the pool

The parabola shape of the velocity plot was unexpected. This can be explained by the boundary setting of the 2D model. The current setting of the bottom end of the pool was ‘out flow’. However, a setting of ‘slip’ should be applied due to the actually deceives. But in order to solve the 2D problem in Femlab, the bottom end of the pool must set up as ‘out flow’, otherwise there will be flow into the model, but no way out, which would cause failure of solving the problem. But we do expected the velocity would be linear behavior for the actually device.

(Note added by instructor: the parabolic profile shown in Fig. 6 is due entirely to the boundary conditions on the side walls, which were taken as no slip. If the simulation were done using a slip boundary, the velocity would have a flat profile.)

Another assumption is that the pressure drop along the micro-jet would be much greater compare to the pressure drop in the side-channel, from the outer boundary to the inner boundary. To approve this, Fig 7 was given.

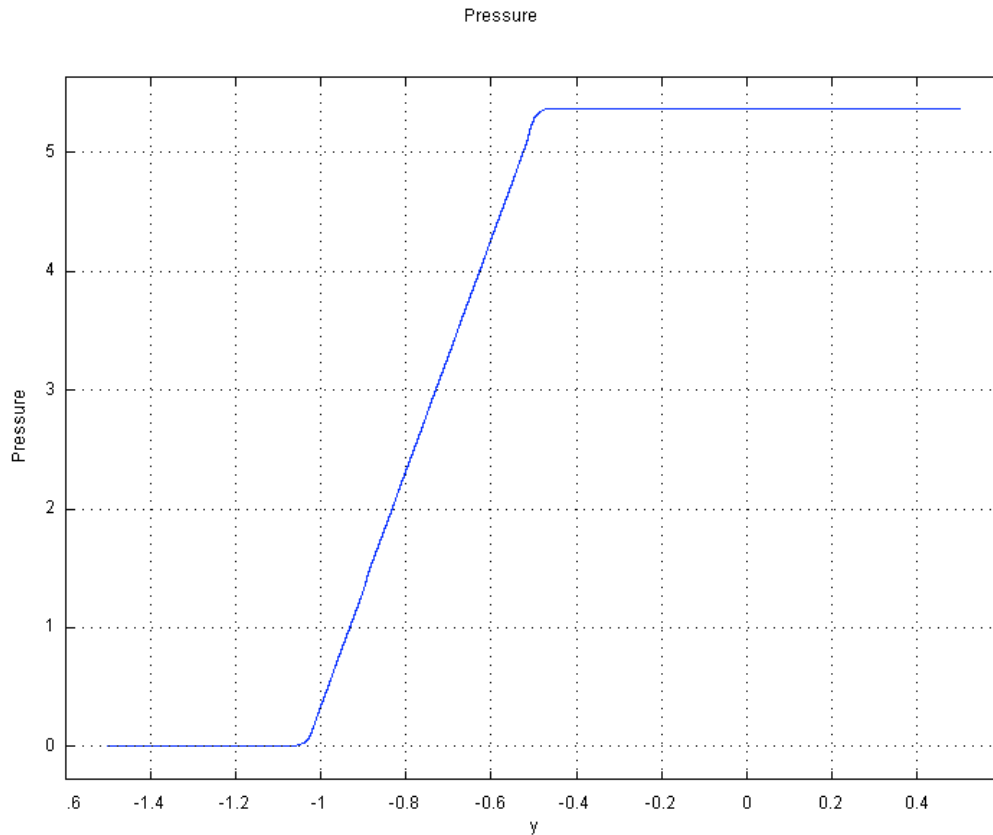


Fig 7. Pressure vs. Position from outer boundary of side-channel through the micro-jet

The horizontal line at the beginning and the end of the plot suggest that the cross channel pressure drop were relatively small compare to the pressure along the micro-jet.

It is also important to discover the fully developed condition of the flow in the side-channel. We assumed the flow enter the side-channel were fully developed. Fig 8 below represents the velocity profile around the entry of side-channel.

x-velocity

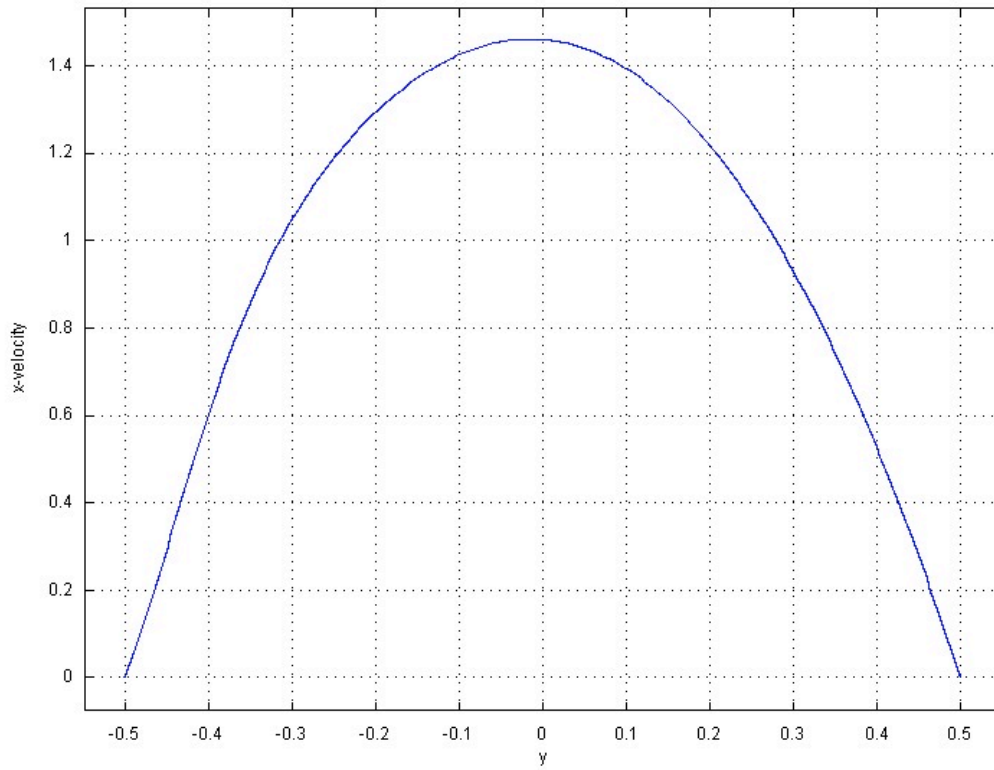


Fig 8. Velocity vs. position near the side-channel entry

The parabola shape of the velocity plot suggests the fully developed condition for the inlet flow. Fig 9 below shows the velocity profile after the first micro-jet.

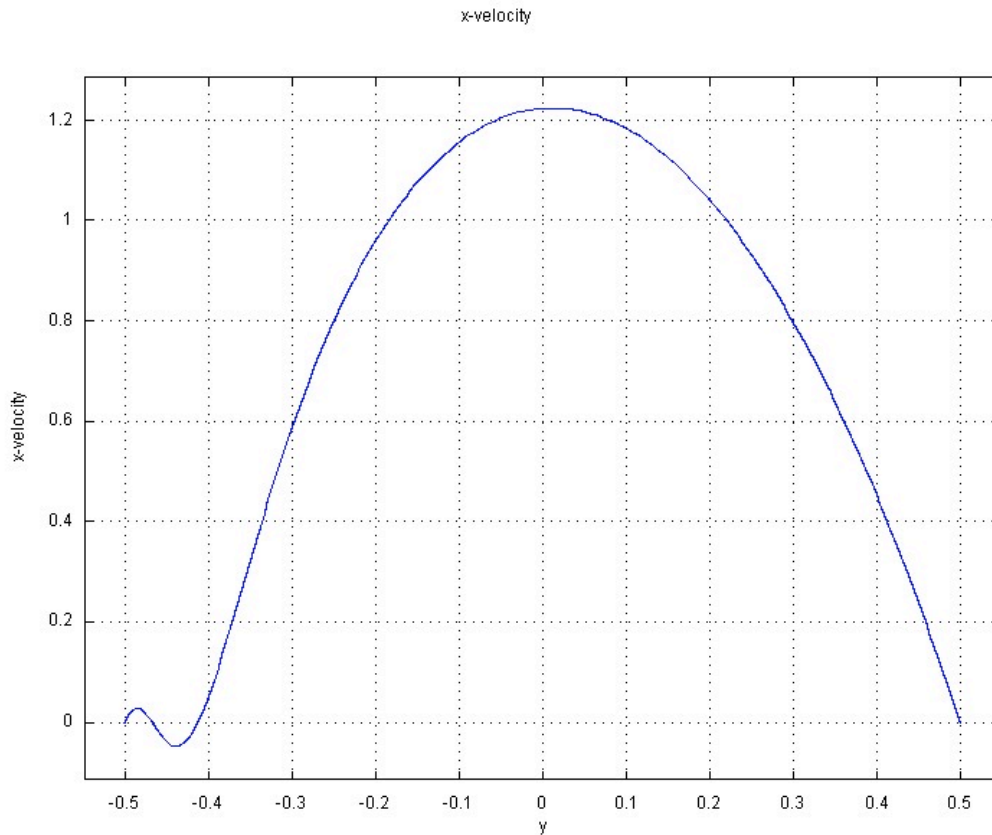


Fig 9. Velocity vs. position after the first micro-jet

It is obvious that the flow did not take a long time to recover to fully developed condition.

Base on these two plots; we can keep the assumption of fully developed flow in side-channel for the rest of study.

3D simulation

Base on the 2D model, a 3D model was demonstrated by Femlab also. Fig 10 below shows the 3D model in Femlab, with 113914 degree of freedom and 24800 elements.

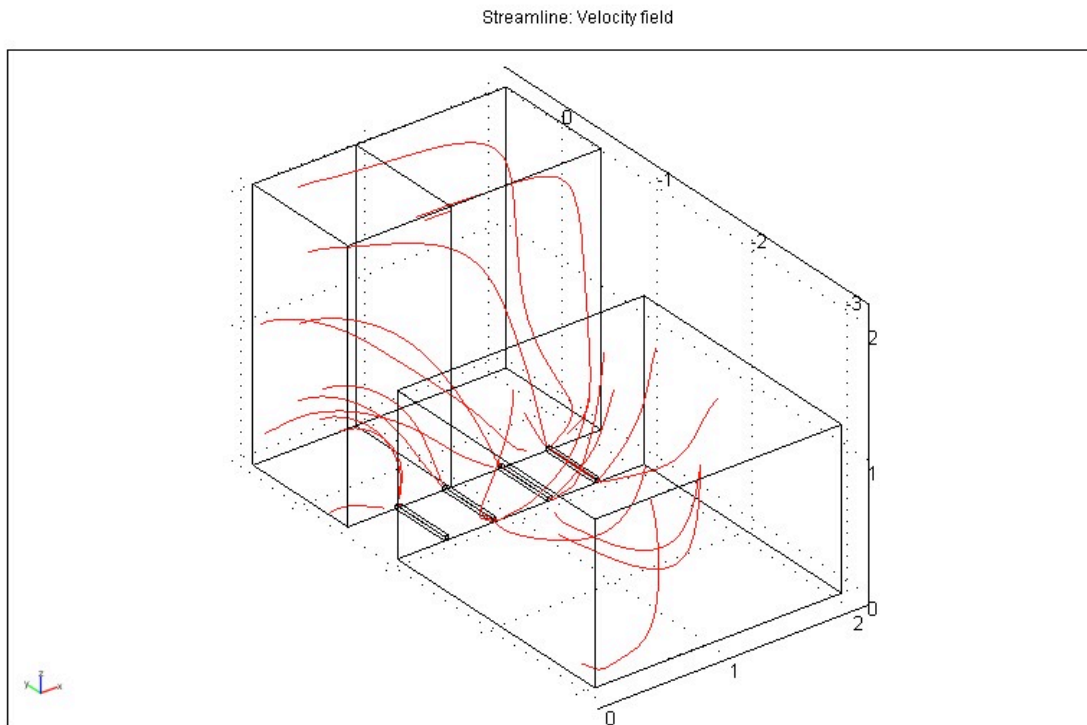


Fig 10. 3D model in Femlab

Boundary set up of the 3D model was very similar to the 2D one. In addition, we can set the other end of pool as “slip” and the top surface of the pool as the “out flow”. These modifications can generate more accurate result base on the actual condition of the device. First of all, the 3D model proves the prediction of linear velocity around the other end of pool. Second, it is useful to study the sheer stress at the bottom of the pool. Fig 11 is the graph of sheer stress at the bottom of the pool.

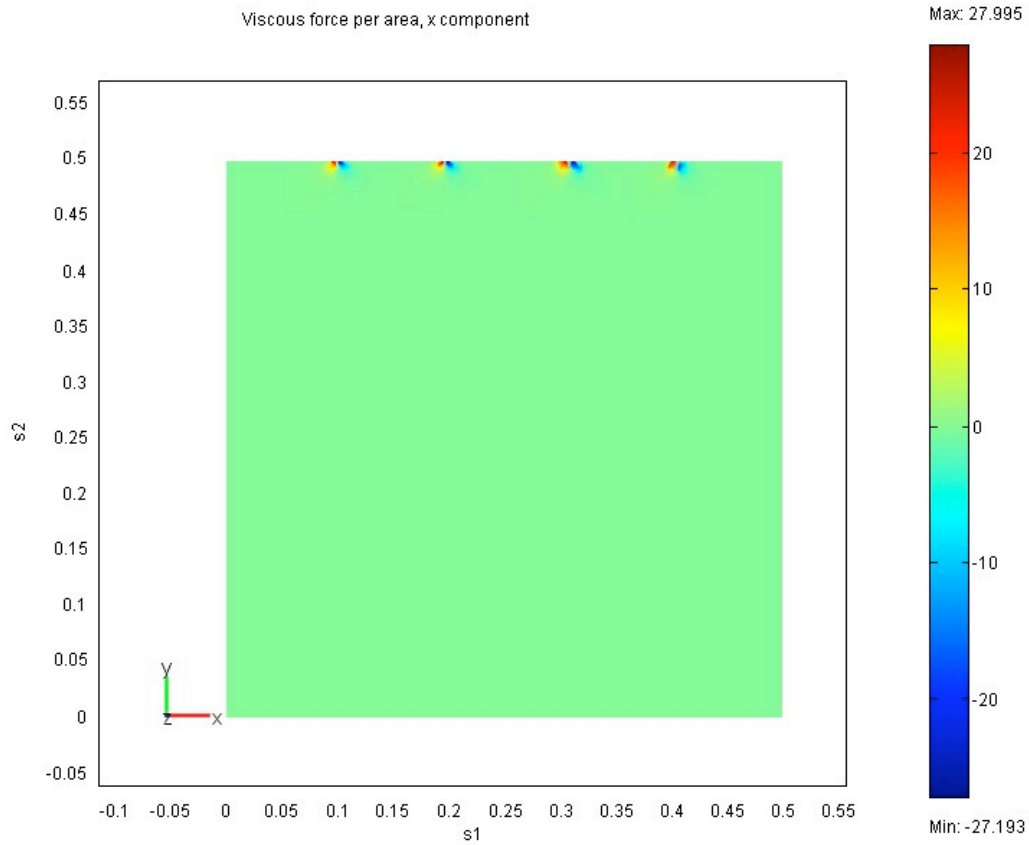


Fig 11. Viscous Force plot

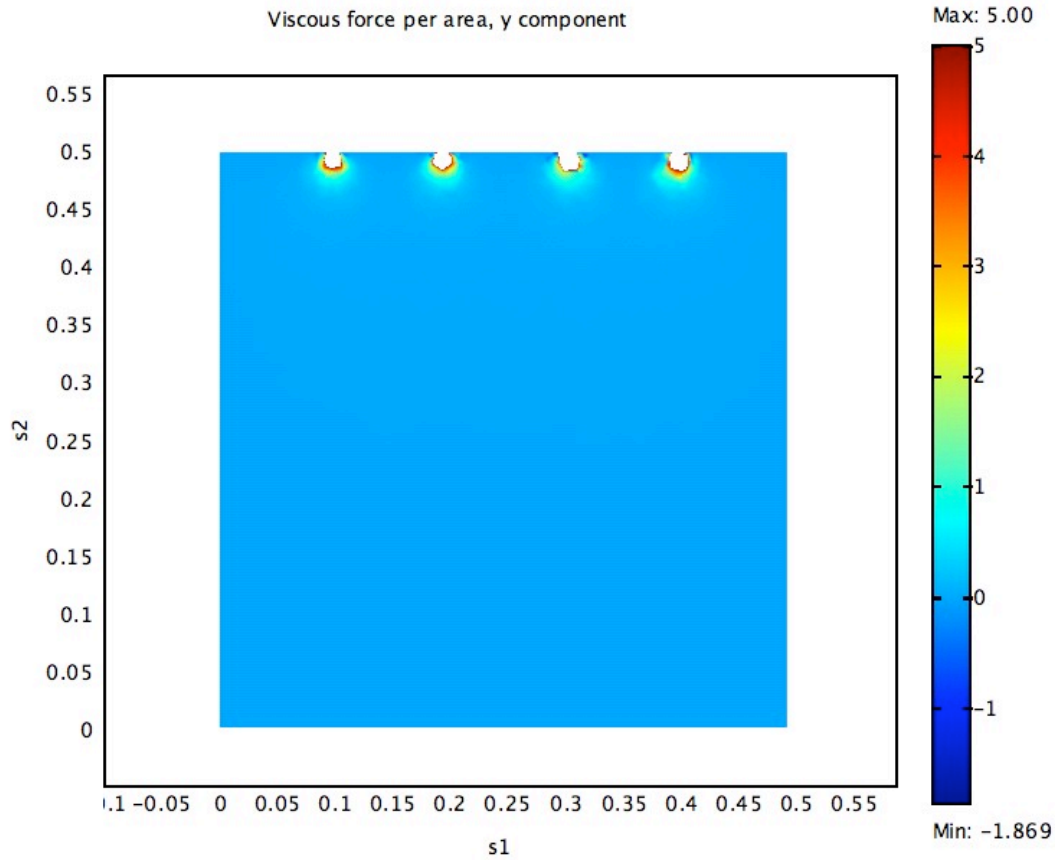


Figure 12. Viscous force using a smaller range for the color scheme.

It is obvious that the greatest force changes occur near the exit of micro-jets. Similarly, the bottom surface of side channel has the greatest force changes near the micro-jet entry. During the experiment, if the brain cell can survive at these points, they should also survive in other locations of the device.

Conclusion

Through the study, the following conclusions can be made:

- Fully developed flowed in side-channels
- Greatest pressure drop occur in the micro-jets
- Velocity and pressure would behave linearly at the center of the pool in actual device
- 3D model consist with 2D model prediction.